SoftwareX 26 (2024) 101716

Contents lists available at ScienceDirect

SoftwareX

journal homepage: www.elsevier.com/locate/softx

Original software publication

Mie–FH: A quantum corrected pair potential in the LAMMPS simulation package for hydrogen mixtures

Thuat T. Trinh [a,*], Morten Hammer [a,c], Vishist Sharma [b], Øivind Wilhelmsen [a,c,*]

[a] Porelab, Department of Chemistry, Norwegian University of Science and Technology - NTNU, NO-7491 Trondheim, Norway
[b] IT Development Section, Norwegian University of Science and Technology - NTNU, NO-7491 Trondheim, Norway
[c] Department of Gas Technology, SINTEF Energy Research, NO-7465 Trondheim, Norway

ARTICLE INFO

Keywords:
Molecular simulations
LAMMPS
Quantum correction
Pair potential
Hydrogen
Feynman Hibbs
Mie

ABSTRACT

Several knowledge gaps on the properties and behavior of hydrogen must be closed to realize its widespread use as a clean fuel and reduction agent. A challenge in this regard is that hydrogen and its mixtures are influenced by quantum effects, in particular at low temperatures. We have implemented new pair potentials into the Large-scale Atomic/Molecular Massively Parallel Simulator (LAMMPS) package that semi-classically account for quantum effects. They are called Feynman–Hibbs corrected Mie potentials (Mie–FH) of first and second order. In the literature, these potentials have been shown to accurately represent the thermodynamic properties of hydrogen, deuterium, helium, neon and their mixtures at temperatures above 20 K. We verify the correctness of the LAMMPS implementation by comparing to results from independent Monte Carlo simulations. The computational efficiency of the implementation is assessed for system sizes ranging from several thousands to one billion particles, highlighting the suitability of the implementation for large-scale simulations. The LAMMPS implementation paves the way for new applications, such as studying the transport properties of hydrogen mixtures, or investigating hydrogen confined in porous media.

Code metadata

Current code version	v 0.1
Permanent link to code/repository used for this code version	https://github.com/ElsevierSoftwareX/SOFTX-D-24-00017
Permanent link to Reproducible Capsule	For example: https://github.com/thermotools/lammps_mie_fh
Legal Code License	MIT
Code versioning system used	git
Software code languages, tools, and services used	C++
Compilation requirements, operating environments & dependencies	GNU, Intel compiler
If available Link to developer documentation/manual	thermotools https://github.com/thermotools
Support email for questions	thuat.trinh@ntnu.no

1. Motivation and significance

Predicting thermo-physical properties is essential for understanding complex systems involving phase transitions, chemical reactions, transport phenomena, and macroscopic behaviors observed in real-world applications [1–8]. Accurate prediction models are indispensable tools for designing efficient processes, optimizing energy utilization, developing new materials, and assessing environmental impacts associated with fluid systems.

The study of thermo-physical properties of fluids with molecular dynamics (MD) simulations has gained significant attention due to its ability to accurately predict various properties, such as phase diagrams, transport coefficients, and free energy exploration. For example, the two-phase thermodynamic model (2PT) [9–13] is an approach for calculating the thermodynamic properties of fluids from single MD simulation trajectories. Another MD study with modeling of thermal conductivity enhancement in metal nanoparticle suspensions was reported by Sankar et al. [14].

* Corresponding authors at: Porelab, Department of Chemistry, Norwegian University of Science and Technology - NTNU, NO-7491 Trondheim, Norway.
E-mail addresses: thuat.trinh@ntnu.no (Thuat T. Trinh), oivind.wilhelmsen@ntnu.no (Øivind Wilhelmsen).

https://doi.org/10.1016/j.softx.2024.101716
Received 12 January 2024; Received in revised form 9 March 2024; Accepted 25 March 2024
Available online 3 April 2024

There are several software packages available to perform MD simulations such as GROMACS [15], AMBER [16], OPENMM [17], DESMOND [18], LAMMPS [19]. Among these packages, LAMMPS is one of the most suitable for material simulations and for studying thermodynamics and transport properties of fluids [19]. The flexibility of LAMMPS [19], which enables custom potential functions and properties tailored to specific needs, makes it particularly suitable for incorporating new potentials in MD simulations. Other notable works in this field include the development of the MD program ms2 by Deublein et al. [20], which is designed for calculating thermodynamic properties of bulk fluids.

Quantum nuclear effects (QNE) play a crucial role in accurately modeling the behavior and properties of molecules at the nanoscale level, particularly when considering systems involving hydrogen-based materials. Hydrogen's lightweight nature amplify nuclear effects on its protons. For example, utilizing experimental techniques like deep inelastic neutron scattering have allowed researchers to probe the quantum nature of water's hydrogen bonds directly [21]. The importance of QNE in the hydrogen liquefaction process has been discussed [22]. This process plays a pivotal role in various industrial applications such as fuel cells, metallurgical processes, and chemical reactions.

To include QNE in classical MD simulations, the package i-Pi [23] provides an interface for other softwares with path integral MD (PIMD). PIMD generates the quantum–mechanical ensemble of a system of interacting particles by using MD in an extended phase space. This is derived from the path integral formalism [24], which relates the statistics of a collection of quantum particles to those of a set of classical ring polymers [25], a ring polymer being a number of replicas of a particle coupled by harmonic springs. An alternative approach to incorporate QNE into MD simulations involves utilizing the quantum thermal bath scheme proposed by Dammak et al. [26]. This method employs a colored thermostat to account for QNE, allowing it to be seamlessly integrated with other time integration schemes within LAMMPS.

In this work, we will present a novel implementation of Feynman–Hibbs corrected Mie potentials (Mie–FH) in LAMMPS. This approach provides an alternative method, distinct from the PIMD (fix pimd) [24] and quantum thermal bath (fix qtb) [26] schemes, for effectively incorporating quantum effects into LAMMPS simulations. Unlike the quantum thermal bath scheme [26], which modifies the thermostat to account for QNE, the Mie–FH approach directly alters the pair potential functional to account for quantum effects. The Mie–FH potentials have been shown to successfully represent the thermodynamic properties of hydrogen, helium, neon, deuterium and their mixtures at temperature above 20 K [27–29].

The successful incorporation of Mie–FH into LAMMPS offers researchers a powerful tool for studying atomic interactions in mixtures that are highly relevant for closing knowledge gaps to realize widespread use of hydrogen as a clean fuel and reduction agent. The implementation can facilitate accurate predictions of phase transitions, structural transformations, and other material properties under varying conditions.

2. Software description

2.1. Software architecture

In this section, we provide a brief overview of how the quantum corrected Mie–FH potential [27] was implemented into the widely used LAMMPS simulation package. This new implementation includes both Mie–FH1 (first order) and Mie–FH2 (second order) variants of the pair potential, along with an additional temperature parameter input that renders the native pair potential temperature dependent. For more details on the theoretical foundation underpinning the Mie–FH potential, readers are encouraged to consult the literature (see [24,27,29] and the references therein).

The Mie–FH pair potential between Fluid i and j is:

$$\begin{aligned}\frac{u_{ij}(r_{ij})}{C(\gamma_{r,ij},\gamma_{a,ij})\epsilon_{ij}} =& \frac{\sigma_{ij}^{\gamma_{r,ij}}}{r_{ij}^{\gamma_{r,ij}}} - \frac{\sigma_{ij}^{\gamma_{a,ij}}}{r_{ij}^{\gamma_{a,ij}}} \\ &+ D\left(Q_1(\gamma_{r,ij})\frac{\sigma_{ij}^{\gamma_{r,ij}+2}}{r_{ij}^{\gamma_{r,ij}+2}} - Q_1(\gamma_{a,ij})\frac{\sigma_{ij}^{\gamma_{a,ij}+2}}{r_{ij}^{\gamma_{a,ij}+2}}\right) \\ &+ D^2\left(Q_2(\gamma_{r,ij})\frac{\sigma_{ij}^{\gamma_{r,ij}+4}}{r_{ij}^{\gamma_{r,ij}+4}} - Q_2(\gamma_{a,ij})\frac{\sigma_{ij}^{\gamma_{a,ij}+4}}{r_{ij}^{\gamma_{a,ij}+4}}\right),\end{aligned} \tag{1}$$

where γ_r and γ_a are the repulsive and attractive exponents of the Mie potential, r_{ij} is the distance, ϵ_{ij} is the Mie well-depth, σ_{ij} is the characteristic length scale corresponding to the distance at which the Mie interparticle potential is zero. The pre-factor of the quantum corrections is

$$D = \frac{\beta\hbar^2}{12 m_{ij}\sigma_{ij}^2}, \tag{2}$$

where $m_{ij}^{-1} = \frac{1}{2}(m_i^{-1} + m_j^{-1})$, m is the particle mass, $\beta = \frac{1}{k_B T}$, k_B is Boltzmann's constant and $\hbar = \frac{h}{2\pi}$ is the reduced Planck's constant. The factors C, Q_1 and Q_2 are

$$C(\gamma_r,\gamma_a) = \left(\frac{\gamma_r}{\gamma_r-\gamma_a}\right)\left(\frac{\gamma_r}{\gamma_a}\right)^{\frac{\gamma_a}{\gamma_r-\gamma_a}}, \tag{3}$$

$$Q_1(\gamma) = \gamma(\gamma-1), \tag{4}$$

$$Q_2(\gamma) = \frac{1}{2}(\gamma+2)(\gamma+1)\gamma(\gamma-1). \tag{5}$$

The original formulation of the Mie potential (line one of Eq. (1)) does not account for quantum effects. However, by incorporating the quantum corrections, the Mie–FH1 (add line two of Eq. (1)) and Mie–FH2 (add also line three of Eq. (1)), the pair potentials are capable of accurately representing the quantum effect of light atoms at low temperatures, while maintaining computational efficiency.

In the LAMMPS implementation, we compute the coefficient parameters (such as C, D, Q1, and Q2) with an explicit temperature input that directly influences the behavior the quantum corrected pair potentials. This approach allows users to more easily account for quantum effects in their MD simulations, while still benefiting from the user friendly input of LAMMPS.

2.2. Software functionalities

The main extension of the Mie–FH is to offer more accurate intermolecular interactions in LAMMPS that still maintain a relatively high computational efficiency. The implementation significantly expands the scope of applicability for computational material science studies involving light elements such as gases and liquids of hydrogen, helium, neon, deuterium and their mixtures. This enables an enhanced capability to calculate thermodynamic properties, vapor–liquid equilibria (VLE), and transport properties (thermal conductivity, diffusion coefficients and viscosities) with greater accuracy for fluids with low molecular masses like hydrogen, helium, and neon.

It should be noted that this potential has certain limitations. As a temperature-dependent potential, the Mie–FH method is well suited for simulations conducted under constant temperature conditions such as NVT (constant number of particles, volume, and temperature) and NPT (constant number of particles, pressure, and temperature). However, non-equilibrium molecular dynamics (NEMD) simulations can have a temperature gradient within the simulation volume. The Mie–FH potential does not currently support these types of calculations directly. As such, researchers interested in studying systems with temperature gradients need to explore alternative methods or modify the existing Mie–FH implementation. Furthermore, since the Feynman–Hibbs corrections approximate quantum effects in a semi-classical manner

and results from a high-temperature expansion [24], they become inaccurate at very low temperatures (Typically below 20 K with the parameters from Refs. [27,29]). The Mie–FH exhibits broad applicability across various temperatures for both liquid and gaseous systems [27, 29]. However, to fully explore its capabilities, it is essential to verify this approach for solid-state conditions, especially under extreme high-pressure scenarios where quantum effects significantly influence material behavior [30].

2.3. Sample code snippets analysis

To take full advantage of the new quantum corrected Mie–FH potential implemented into LAMMPS, users are encouraged to download the source code from the dedicated GitHub repository (https://github.com/thermotools/Mie-FH). For a comprehensive understanding of the specific implementation details of the Mie–FH model, we invite the readers to explore the source code files within the EXTRA-PAIR folder, which contains all necessary modifications and integration of quantum corrections. Once the code has been successfully cloned and compiled according to the standard LAMMPS routine, researchers can begin exploring examples with molecular simulations.

The new pair potentials have been named "pair Mie-FH1/cut" and "pair Mie-FH2/cut" for ease of use within MD simulations. It is important to note that the pair Mie–FH supports long-range tail corrections for energy and pressure. An example input script for hydrogen gas has also been provided on the GitHub repository to demonstrate how these force fields can be incorporated into existing LAMMPS simulation protocols. A complete documentation of the Mie–FH potential is also provided in the source code. An example of how to download and use the code is presented below:

```
(get the code with download .zip or git clone)
git clone https://github.com/thermotools/lammps_mie_fh
cd lammps_mie_fh
cd src
make yes-extra-pair
make yes-molecule
make mpi
mpirun -np 4 lmp_mpi -in ../Mie-FH1-npt.lmp
```

3. Simulation examples

3.1. Comparison with the Monte Carlo simulations

First we present a comparative analysis between results generated by using the new Mie–FH implementation in LAMMPS combined with MD simulations, and results generated by using the independent Monte Carlo (MC) simulation code used in Refs. [27,29]. A system containing 4000 particle was selected (Fig. 1) and two variants of the Mie–FH potential were tested: Mie–FH1 and Mie–FH2 with parameters described in Table 1. We have chosen parameters that mimic the behavior of hydrogen. The MC simulations were carried out with a fixed number of particles N, pressure P and temperature T (NPT-ensemble) using the arrays of values listed in Table 1. We also selected the NPT option for the MD simulation in LAMMPS.

Fig. 2 shows that the calculated densities obtained from LAMMPS with the implemented Mie–FH potential are in excellent agreement with those computed with the MC code. It is worth mentioning that the typical error bars associated with density calculations in MD simulations using the Mie–FH potential are generally within the range of 1%–3% of the expected values. This validates the implementation of the quantum corrected pair potential Mie–FH within the MD framework and highlights its potential for enhancing our understanding of atomic interactions in various materials systems where quantum effects are important.

It is important to note that LAMMPS offers a distinct advantage over Monte Carlo methods by enabling the computation of dynamical properties, which play a crucial role in elucidating and characterizing fluid behavior in diverse applications.

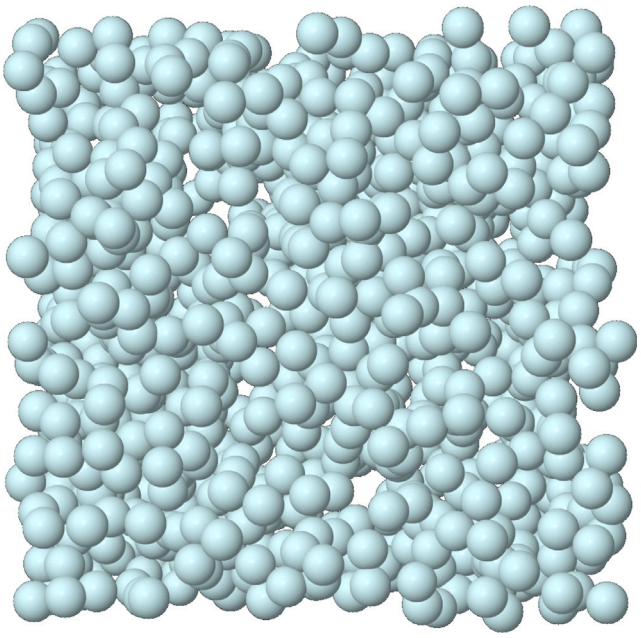

Fig. 1. Snapshot from the MD simulations of a system containing 4000 particles. The visual representation of the system was prepared with the VMD software [31].

Table 1
Potential parameters for Mie–FH1 and Mie–FH2 for hydrogen [27], together with the cut-off radius r_{cut}, temperatures T and pressures P considered when comparing Lammps Mie–FH to the original MC code used in Refs. [27,29].

Pair potential	σ (Å)	r_{cut} (Å)	ϵ (kB)	γ_r	γ_a	T (K)	P (Pa)
Mie–FH1	2.74	12.33 (4.5σ)	5.42	9	6	75	5.00E+05
						75	3.00E+06
						75	1.00E+07
						100	5.00E+05
						100	3.00E+06
						100	1.00E+07
						50	5.00E+05
						50	3.00E+06
						50	1.00E+07
Mie–FH2	3.0	13.5	30.0	24	6	30	1.53E+07
						40	1.53E+07
						50	1.53E+07
						60	1.53E+07

3.2. Benchmark and scaling

In order to evaluate the computational performance of the implemented Mie–FH potential within the LAMMPS simulation package, we conducted a series of benchmark studies with system sizes ranging from several thousands to one billion atoms. These simulations were designed to study various physical properties and behaviors under different conditions, with a particular focus on phase transitions, structural transformations, and material performance scaling. The benchmarking of scalability was conducted by using the Norwegian Sigma2 supercomputers Betzy [32] with up to 128 nodes with around 16k cores. The box length (L) and total memory requirements for each benchmark system are listed in Table 2.

As the benchmark studies progressed, we encountered a significant computational challenge when attempting to simulate systems containing one billion particles. The so-called *Giant* systems pose unique challenges due to their immense memory requirements, which can exceed several terabytes for even relatively simple molecular configurations (as evidenced by the 1.7 TB total memory requirement listed in Table 2). Given the prohibitive nature of these computational demands, it becomes apparent that traditional desktop or laptop computers are ill-equipped to handle such simulations.

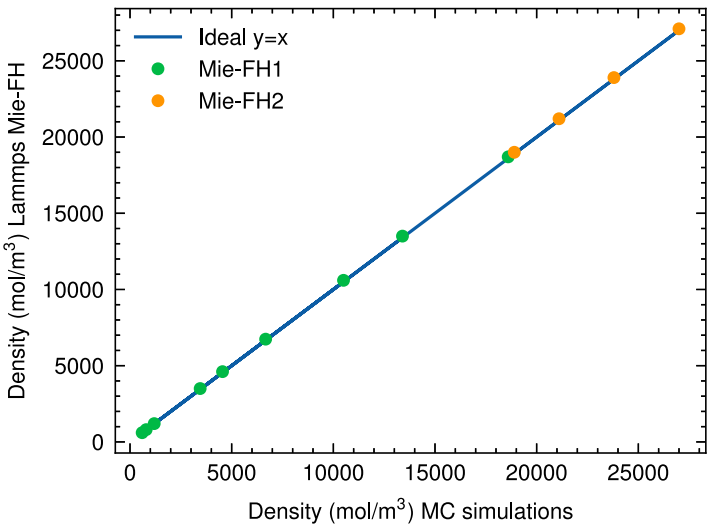

Fig. 2. Comparison of the density obtained from LAMMPS with the implemented Mie–FH pair potentials with results from an MC code that was used to generate the results in Refs. [27,29]. The details of the systems can be found in Table 1.

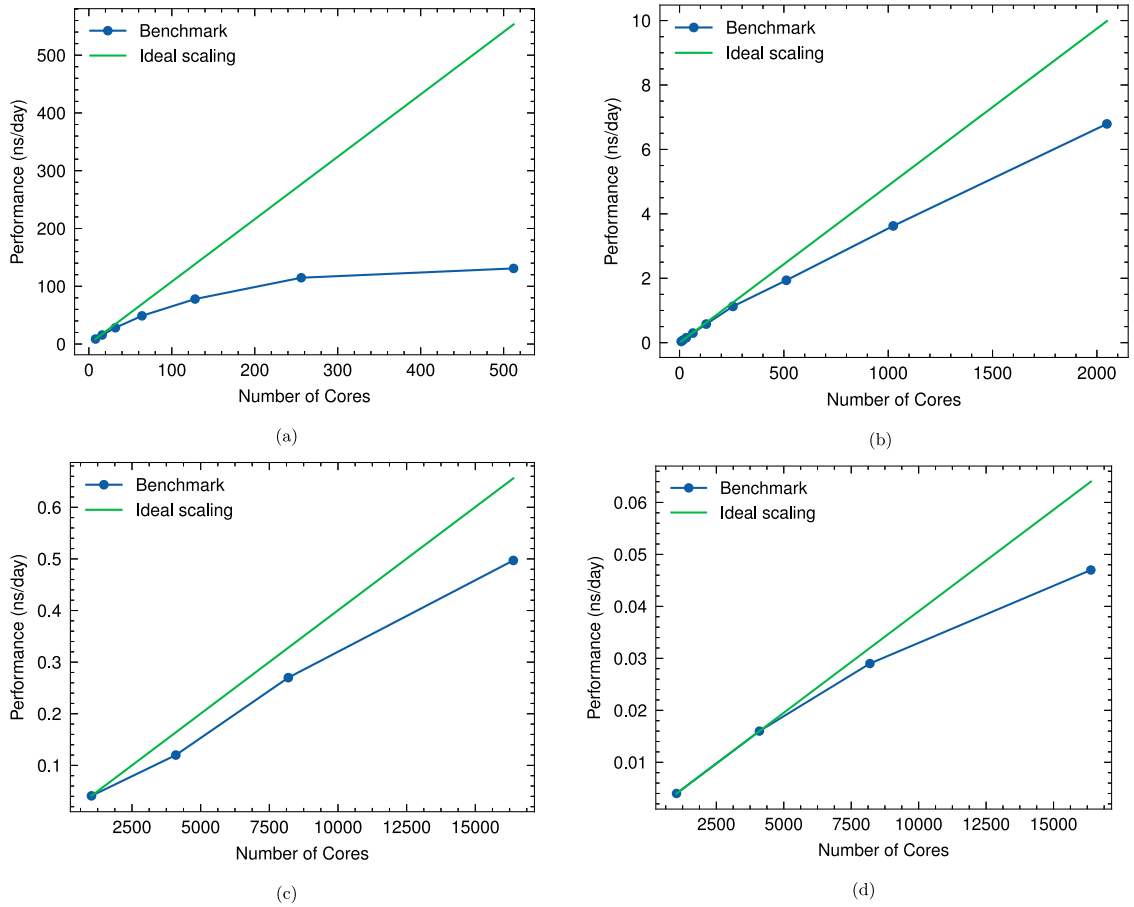

Fig. 3. Performance of different benchmark systems using LAMMPS Mie–FH2. The results are from Small (a), Big (b), Huge (c) and Giant (d), as defined in Table 2.

To gain a deeper understanding of how the Mie–FH potential performs under various computational conditions, we conducted an extensive performance scaling analysis as illustrated in Fig. 3. The graph depicts the relationship between the performance (in terms of nanoseconds per day), and the number of cores utilized for each simulation.

As expected, the results show that increasing the number of cores can improve the overall performance. However, for the *small* system with 4000 atoms, we observe that after using 64 cores, increasing the number of cores failed to yield any substantial speedup. The performance actually decreases in this system due to increased communication overhead and reduced parallelization efficiency.

When utilizing MD simulations, one must strike a balance between system size and performance. While smaller systems can achieve simulation speeds of hundreds of ns/day, larger systems with billions of

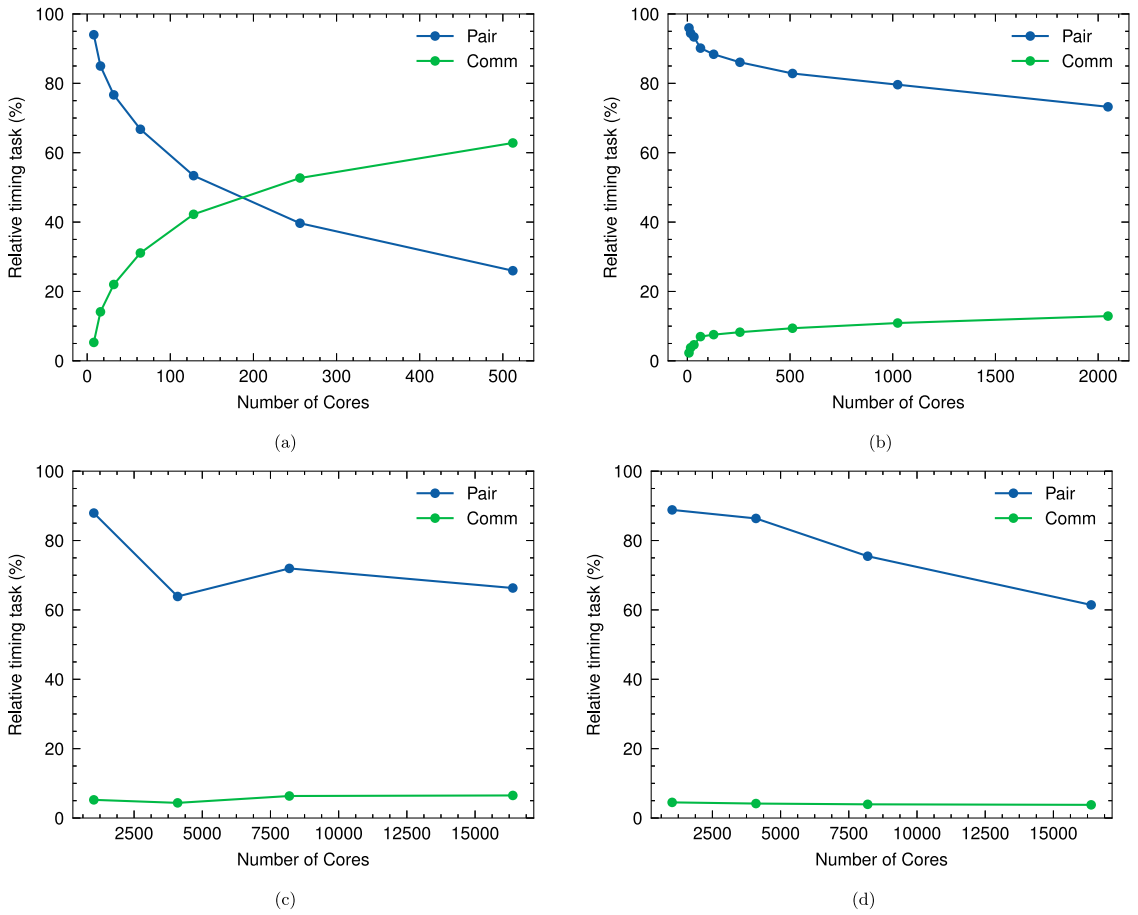

Fig. 4. Analysis of timing tasks for computing pair (Pair) and MPI communication time (Comm) of different benchmark systems using LAMMPS Mie–FH2. The results are from Small (a), Big (b), Huge (c) and Giant (d), as defined in Table 2.

Table 2
Different system sizes ranging from several thousands to one billion particles for studying benchmark and performance scaling. The box length (L) and total memory requirements are also listed.

System name	N	L (nm)	Memory (GB)
Small	4.0E+03 (4k)	5.0	0.75
Large	1.0E+06 (1M)	31.5	14.66
Huge	1.0E+08 (100M)	146.0	265.68
Giant	1.0E+09 (1B)	315.0	1739.20

atoms may see significant reductions in performance, dropping down to just 0.01 ns/day, even using a large supercomputer. This trade-off highlights the importance of carefully selecting system size and computational resources based on the specific research questions being investigated. In some cases, supercomputers or HPC clusters may be necessary to achieve meaningful results within reasonable timeframes for large-scale systems.

To further elucidate the performance characteristics of the MD simulations, we conducted a detailed task-level analysis focusing on two key metrics: computational time of pairwise interactions (Pair) and communication overhead associated with exchanging information between processors (Comm). Since OpenMP was not used in the benchmark study, the time of communication was only from the Message Passing Interface (MPI) for sending and receiving messages between processors. The results are presented in Fig. 4.

As expected, the findings reveal that increasing the number of cores leads to a concurrent reduction in the percentage of compute time used for calculating pairwise interactions. For example in the system with 4000 particles, we observe an increase in communication time due to the higher volume of messages being sent and received between processors — a phenomenon often referred to as "communication bottleneck". For the *small* system, it was observed that after reaching roughly 180 cores, the simulation began spending more time on communication between MPI threads than actually computing pair interactions. This finding emphasizes the importance of carefully selecting the number of cores used in MD simulations to avoid unnecessary overheads and optimize performance for a given system size.

In contrast to smaller systems, larger MD simulations with millions and billions of atoms exhibit relatively lower communication times compared to the computational effort required for pairwise calculations. As the system size increases, a greater proportion of overall simulation time is dedicated to computing interatomic interactions between particles. This results in a more even distribution of workload across available cores and reduced need for extensive communication between MPI threads.

The benchmark for the Mie–HF potential on an AMD CPU platform (Betzy supercomputer) could guide potential users in selecting suitable simulation parameters. Interestingly, we observed no impact of including quantum nuclear effects on the performance of the Mie potential. Both Mie/cut and Mie–FH/cut pair performances remain comparable, demonstrating the robustness of the implementation.

The comprehensive analysis of efficiency trends and optimization strategies highlights the complex interplay between computational algorithms, parallelization techniques, and system size when working with advanced MD simulation packages like LAMMPS. By striking a balance between these competing factors, researchers can continue to push the boundaries of what is computationally feasible while simultaneously gaining new insights and making new discoveries across diverse scientific disciplines.

4. Impact

The successful implementation of the quantum corrected Mie–FH potential into the widely used LAMMPS simulation package opens up several new avenues for exploration within the realm of MD simulations. As researchers continue to push the boundaries of what is computationally feasible, several new research questions and challenges emerge that can be pursued as a result of this implementation. It is noteworthy that the Mie–FH potential is fully compatible with the MD simulations, enabling its seamless integration with advanced methods like the multi-timestep integrators implemented in LAMMPS for enhanced simulation efficiency and accuracy.

The ability of these potentials to accurately represent the intermolecular interactions and thermodynamic properties of fluids such as hydrogen, helium, neon, deuterium and the mixtures has been demonstrated in previous work [27–29]. Using advanced quantum corrected force fields like Mie–FH offers new opportunities to study the behavior of these fluids also at conditions that are experimentally inaccessible. Moreover, their ability to represent transport properties such as diffusion coefficients [33], thermal conductivities and viscosities can be leveraged to close present knowledge gaps on hydrogen transport [34–36], and reaction thermodynamics [37–39].

In future research, the LAMMPS implementation can contribute to characterize the thermo-physical properties of novel mixed refrigerant mixtures that have the potential to enhance the energy efficiency of the hydrogen liquefaction process [22,40,41], where vapor–liquid and liquid–liquid equilibria are central [42,43]. Furthermore, researchers can develop more accurate equation of state models [44] for predicting the performance characteristics of energy conversion systems such as fuel cells [45], solar panels, or electrochemical batteries.

Hence, the integration of the Mie–FH into the widely used LAMMPS package represents a significant contribution that is likely to be of societial importance. By combining LAMMPS' extensive capabilities for material simulations with the possibilities provided by the Mie–FH potential, researchers can now make progress on a wide range of challenges.

5. Conclusions

Feynman–Hibbs corrected Mie potentials (Mie–FH) of first (Mie–FH1) and second order (Mie–FH2) have been implemented into the popular Large-scale Atomic/Molecular Massively Parallel Simulator (LAMMPS) package. These potentials account for quantum effects in a semi-classical manner that makes the interaction potentials depend on temperature. In the literature, Mie–FH potentials have been shown to be capable of accurately represent the thermodynamic properties of hydrogen, helium, neon, deuterium and their mixtures at temperatures above 20 K. The correctness of the implementation of these potentials in LAMMPS was verified by confirming that the results agreed with results obtained from an independent Monte Carlo code that has been validated in previous work.

Benchmarking tests were conducted across a wide range of system sizes, ranging from several thousands up to one billion atoms. These tests confirmed the computational efficiency and scalability of the new pair styles (Mie–FH1 and Mie–FH2) within LAMMPS. To optimize performance when utilizing this novel implementation, it is recommended that users adjust the number of cores based on their system size to minimize communication time between MPI threads. Large numbers of cores for small systems might not be efficient due to the increased communication overhead.

While the current study focuses on the implementation of the Mie–FH model within LAMMPS and benchmarking of different system sizes, we recognize that extensive simulations exploring transport properties and comparisons with other force fields are essential. In future research, we aim to develop a GPU-accelerated version of the Mie–HF potential, which has the potential to substantially enhance simulation performance for large systems and complex fluids by leveraging the parallel processing capabilities of graphics processing units.

The implementation of the Mie–FH potentials in LAMMPS provides a valuable tool for researchers studying the thermodynamic properties of hydrogen, helium, neon, deuterium and their mixtures. Furthermore, the implementation paves the way for new applications, such as studying the transport properties of hydrogen mixtures, or investigating hydrogen confined in porous media.

CRediT authorship contribution statement

Thuat T. Trinh: Writing – review & editing, Writing – original draft, Supervision, Conceptualization, Data curation, Methodology. **Morten Hammer:** Software, Investigation, Formal analysis, Data curation, Methodology. **Vishist Sharma:** Software, Methodology, Investigation, Data curation. **Øivind Wilhelmsen:** Writing – review & editing, Validation, Funding acquisition, Conceptualization.

Declaration of competing interest

The authors declare that they have no known competing financial interests or personal relationships that could have appeared to influence the work reported in this paper.

Data availability

Data will be made available on request.

Acknowledgments

We would like to thank the AUS (Advanced User Support) from Research Council of Norway and Sigma2. TTT, MH and ØW acknowledge funding from the Research Council of Norway (RCN), the Center of Excellence Funding Scheme, Project No. 262644, PoreLab. The publication has been partially funded by The Research Council of Norway and produced under the project No 327056 Monitoring and Control of CCS networks – MACON CCS.

References

[1] Larsen BL, Rasmussen P, Fredenslund A. A modified UNIFAC group-contribution model for prediction of phase equilibria and heats of mixing. Ind Eng Chem Res 1987;26(11):2274–86. http://dx.doi.org/10.1021/ie00071a018.

[2] Duangthongsuk W, Wongwises S. Measurement of temperature-dependent thermal conductivity and viscosity of TiO2-water nanofluids. Exp Therm Fluid Sci 2009;33(4):706–14. http://dx.doi.org/10.1016/j.expthermflusci.2009.01.005.

[3] Smith R. A scheme for predicting layer clouds and their water content in a general circulation model. Quart J Royal Meteoro Soc 1990;116(492):435–60. http://dx.doi.org/10.1002/qj.49711649210.

[4] Tang I, Munkelwitz H. Water activities, densities, and refractive indices of aqueous sulfates and sodium nitrate droplets of atmospheric importance. J Geophys Res 1994;99(D9):18801–8. http://dx.doi.org/10.1029/94jd01345.

[5] Dey D, Kumar P, Samantaray S. A review of nanofluid preparation, stability, and thermo-physical properties. Heat Trans Asian Res 2017;46(8):1413–42. http://dx.doi.org/10.1002/htj.21282.

[6] Xu L, Dai L, Yin L, Sun X, Xu W, Yang R, et al. Research on the climate response of variable thermo-physical property building envelopes: A literature review. Energy Build 2020;226:110398. http://dx.doi.org/10.1016/j.enbuild.2020.110398.

[7] Fabre E, Murshed SMS. A review of the thermophysical properties and potential of ionic liquids for thermal applications. J Mater Chem A 2021;9(29):15861–79. http://dx.doi.org/10.1039/d1ta03656d.

[8] Tillotson MJ, Diamantonis NI, Buda C, Bolton LW, Müller EA. Molecular modelling of the thermophysical properties of fluids: Expectations, limitations, gaps and opportunities. Phys Chem Chem Phys 2023;25(18):12607–28. http://dx.doi.org/10.1039/d2cp05423j.

[9] Lin S-T, Blanco M, Goddard WA. The two-phase model for calculating thermodynamic properties of liquids from molecular dynamics: Validation for the phase diagram of lennard-Jones fluids. J Chem Phys 2003;119(22):11792–805. http://dx.doi.org/10.1063/1.1624057.

[10] Lin S-T, Maiti PK, Goddard WA. Two-phase thermodynamic model for efficient and accurate absolute entropy of water from molecular dynamics simulations. J Phys Chem B 2010;114(24):8191–8. http://dx.doi.org/10.1021/jp103120q.

[11] Madarász Á, Hamza A, Ferenc D, Bakó I. Two faces of the two-phase thermodynamic model. J Chem Theory Comput 2021;17(11):7187–94. http://dx.doi.org/10.1021/acs.jctc.1c00156.

[12] Sulaimon AA, Falade GK. New two-phase and three-phase thermodynamic models for predicting wax precipitation in hydrocarbon mixtures. J Pet Sci Eng 2022;208:109707. http://dx.doi.org/10.1016/j.petrol.2021.109707.

[13] Guo Y, Chen X, Yu X, Wan J, Cao X. Prediction and validation of monoclonal antibodies separation in aqueous two-phase system using molecular dynamic simulation. J Chromatogr A 2023;1694:463921. http://dx.doi.org/10.1016/j.chroma.2023.463921.

[14] Sankar N, Mathew N, Sobhan C. Molecular dynamics modeling of thermal conductivity enhancement in metal nanoparticle suspensions. Int Commun Heat Mass Transfer 2008;35(7):867–72. http://dx.doi.org/10.1016/j.icheatmasstransfer.2008.03.006.

[15] Abraham MJ, Murtola T, Schulz R, Páll S, Smith JC, Hess B, Lindahl E. GROMACS: High performance molecular simulations through multi-level parallelism from laptops to supercomputers. SoftwareX 2015;1–2:19–25. http://dx.doi.org/10.1016/j.softx.2015.06.001.

[16] Case DA, Cheatham TE, Darden T, Gohlke H, Luo R, Merz KM, et al. The amber biomolecular simulation programs. J Comput Chem 2005;26(16):1668–88. http://dx.doi.org/10.1002/jcc.20290.

[17] Eastman P, Swails J, Chodera JD, McGibbon RT, Zhao Y, Beauchamp KA, et al. OpenMM 7: Rapid development of high performance algorithms for molecular dynamics. PLoS Comput Biol 2017;13(7):e1005659. http://dx.doi.org/10.1371/journal.pcbi.1005659.

[18] Bowers KJ, Chow DE, Xu H, Dror RO, Eastwood MP, Gregersen BA, et al. Scalable algorithms for molecular dynamics simulations on commodity clusters. In: ACM/IEEE SC 2006 conference. SC'06, IEEE; 2006, p. 84–es. http://dx.doi.org/10.1109/sc.2006.54.

[19] Thompson AP, Aktulga HM, Berger R, Bolintineanu DS, Brown WM, Crozier PS, et al. LAMMPS - a flexible simulation tool for particle-based materials modeling at the atomic, meso, and continuum scales. Comput Phys Comm 2022;271:108171. http://dx.doi.org/10.1016/j.cpc.2021.108171.

[20] Deublein S, Eckl B, Stoll J, Lishchuk SV, Guevara-Carrion G, Glass CW, et al. ms2: A molecular simulation tool for thermodynamic properties. Comput Phys Comm 2011;182(11):2350–67. http://dx.doi.org/10.1016/j.cpc.2011.04.026.

[21] Ceriotti M, Fang W, Kusalik PG, McKenzie RH, Michaelides A, Morales MA, et al. Nuclear quantum effects in water and aqueous systems: Experiment, theory, and current challenges. Chem Rev 2016;116(13):7529–50. http://dx.doi.org/10.1021/acs.chemrev.5b00674.

[22] Wilhelmsen Ø, Berstad D, Aasen A, Nekså P, Skaugen G. Reducing the exergy destruction in the cryogenic heat exchangers of hydrogen liquefaction processes. Int J Hydrog Energy 2018;43(10):5033–47. http://dx.doi.org/10.1016/j.ijhydene.2018.01.094.

[23] Kapil V, Rossi M, Marsalek O, Petraglia R, Litman Y, Spura T, et al. i-PI 2.0: A universal force engine for advanced molecular simulations. Comput Phys Comm 2019;236:214–23. http://dx.doi.org/10.1016/j.cpc.2018.09.020.

[24] Feynman RP, Hibbs AR, Styer DF. Quantum mechanics and path integrals. Courier Corporation; 2010.

[25] Markland TE, Manolopoulos DE. An efficient ring polymer contraction scheme for imaginary time path integral simulations. J Chem Phys 2008;129(2). http://dx.doi.org/10.1063/1.2953308.

[26] Dammak H, Chalopin Y, Laroche M, Hayoun M, Greffet J-J. Quantum thermal bath for molecular dynamics simulation. Phys Rev Lett 2009;103(19):190601. http://dx.doi.org/10.1103/physrevlett.103.190601.

[27] Aasen A, Hammer M, Ervik Å, Müller EA, Wilhelmsen Ø. Equation of state and force fields for Feynman–Hibbs-corrected Mie fluids. I. Application to pure helium, neon, hydrogen, and deuterium. J Chem Phys 2019;151(6). http://dx.doi.org/10.1063/1.5111364.

[28] Aasen A, Hammer M, Lasala S, Jaubert J-N, Wilhelmsen Ø. Accurate quantum-corrected cubic equations of state for helium, neon, hydrogen, deuterium and their mixtures. Fluid Phase Equilib 2020;524:112790. http://dx.doi.org/10.1016/j.fluid.2020.112790.

[29] Aasen A, Hammer M, Müller EA, Wilhelmsen Ø. Equation of state and force fields for Feynman–Hibbs-corrected Mie fluids. II. Application to mixtures of helium, neon, hydrogen, and deuterium. J Chem Phys 2020;152(7). http://dx.doi.org/10.1063/1.5136079.

[30] Biermann S, Hohl D, Marx D. Quantum effects in solid hydrogen at ultra-high pressure. Solid State Commun 1998;108(6):337–41. http://dx.doi.org/10.1016/s0038-1098(98)00388-3.

[31] Humphrey W, Dalke A, Schulten K. VMD: Visual molecular dynamics. J Mol Graph 1996;14(1):33–8. http://dx.doi.org/10.1016/0263-7855(96)00018-5.

[32] Betzy; Sigma2 documentation — documentation.sigma2.no. 2023, https://documentation.sigma2.no/hpc_machines/betzy.html. [Accessed 30 December 2023].

[33] Yamabe J, Takakuwa O, Matsunaga H, Itoga H, Matsuoka S. Hydrogen diffusivity and tensile-ductility loss of solution-treated austenitic stainless steels with external and internal hydrogen. Int J Hydrog Energy 2017;42(18):13289–99. http://dx.doi.org/10.1016/j.ijhydene.2017.04.055.

[34] Mine Y, Narazaki C, Murakami K, Matsuoka S, Murakami Y. Hydrogen transport in solution-treated and pre-strained austenitic stainless steels and its role in hydrogen-enhanced fatigue crack growth. Int J Hydrog Energy 2009;34(2):1097–107. http://dx.doi.org/10.1016/j.ijhydene.2008.11.018.

[35] Yang F, Kung S-C, Cheng M, Hemminger JC, Penner RM. Smaller is faster and more sensitive: The effect of wire size on the detection of hydrogen by single palladium nanowires. ACS Nano 2010;4(9):5233–44. http://dx.doi.org/10.1021/nn101475c.

[36] Yamabe J, Awane T, Matsuoka S. Investigation of hydrogen transport behavior of various low-alloy steels with high-pressure hydrogen gas. Int J Hydrog Energy 2015;40(34):11075–86. http://dx.doi.org/10.1016/j.ijhydene.2015.07.006.

[37] Mills G, Jónsson H, Schenter GK. Reversible work transition state theory: Application to dissociative adsorption of hydrogen. Surf Sci 1995;324(2–3):305–37. http://dx.doi.org/10.1016/0039-6028(94)00731-4.

[38] Cashdollar KL, A Zlochower I, Green GM, Thomas RA, Hertzberg M. Flammability of methane, propane, and hydrogen gases. J Loss Prev Process Ind 2000;13(3–5):327–40. http://dx.doi.org/10.1016/s0950-4230(99)00037-6.

[39] Trinh TT, Meling N, Bedeaux D, Kjelstrup S. Thermodynamic properties of hydrogen dissociation reaction from the small system method and reactive force field ReaxFF. Chem Phys Lett 2017;672:128–32. http://dx.doi.org/10.1016/j.cplett.2017.01.058.

[40] Wilhelmsen Ø, Johannessen E, Kjelstrup S. Energy efficient reactor design simplified by second law analysis. Int J Hydrog Energy 2010;35(24):13219–31. http://dx.doi.org/10.1016/j.ijhydene.2010.08.118.

[41] Hånde R, Wilhelmsen Ø. Minimum entropy generation in a heat exchanger in the cryogenic part of the hydrogen liquefaction process: On the validity of equipartition and disappearance of the highway. Int J Hydrog Energy 2019;44(29):15045–55. http://dx.doi.org/10.1016/j.ijhydene.2019.03.229.

[42] Hsieh C-M, Sandler SI, Lin S-T. Improvements of COSMO-SAC for vapor–liquid and liquid–liquid equilibrium predictions. Fluid Phase Equilib 2010;297(1):90–7. http://dx.doi.org/10.1016/j.fluid.2010.06.011.

[43] Hammer M, Bauer G, Stierle R, Gross J, Wilhelmsen Ø. Classical density functional theory for interfacial properties of hydrogen, helium, deuterium, neon, and their mixtures. J Chem Phys 2023;158(10). http://dx.doi.org/10.1063/5.0137226.

[44] Soave G. Equilibrium constants from a modified Redlich–Kwong equation of state. Chem Eng Sci 1972;27(6):1197–203. http://dx.doi.org/10.1016/0009-2509(72)80096-4.

[45] Raka YD, Bock R, Karoliussen H, Wilhelmsen Ø, Stokke Burheim O. The influence of concentration and temperature on the membrane resistance of ion exchange membranes and the levelised cost of hydrogen from reverse electrodialysis with ammonium bicarbonate. Membranes 2021;11(2):135. http://dx.doi.org/10.3390/membranes11020135.